

1 Ocean migration of pop-up satellite archival tagged Atlantic salmon from
2 the Miramichi River in Canada

3

4 John Fredrik Strøm¹, Eva B. Thorstad^{1,2}, Graham Chafe³, Sigrunn H. Sørbye⁴, David
5 Righton⁵, Audun H. Rikardsen¹ and Jonathan Carr³

6

7 ¹Department of Arctic and Marine Biology, UiT The Arctic University of Norway,
8 9037 Tromsø, Norway

9 ²Norwegian Institute for Nature Research (NINA), Høgskoleringen 9, 7034
10 Trondheim, Norway

11 ³Atlantic Salmon Federation, 15 Rankine Mill Road, E5B3A9 Chamcook, NB
12 Canada

13 ⁴Department of Mathematics and Statistics, UiT The Arctic University of Norway,
14 9037 Tromsø, Norway

15 ⁵Centre for Environment, Fisheries and Aquaculture Science (Cefas), Pakefield Road,
16 Lowestoft NR33 0HT, UK

17

18 **Corresponding authors:** Graham Chafe: email: gchafe@asf.ca

19

20 **Keywords:** Acoustic telemetry, Atlantic salmon, diving behaviour, Hidden Markov
21 Model (HMM), marine migration, pop-up satellite archival tags (PSATs).

22 **Abstract**

23

24 The ocean migration of 16 post-spawned adult Atlantic salmon (*Salmo salar* L.) from
25 the Miramichi River, Canada, tagged concurrently with pop-up satellite archival tags
26 and acoustic transmitters was reconstructed using a Hidden Markov Model.
27 Individuals exclusively utilized areas within the Gulf of St. Lawrence and the
28 Labrador Sea, and showed little overlap with known distributions of European stocks.
29 During the migration, individuals were generally associated with surface waters and
30 spent more than 67% of the time in the upper 10 m of the water column. The Atlantic
31 salmon occupied greater depths and showed more diving activity during the day than
32 during the night, with a few exceptions. While residing in the Gulf of St. Lawrence,
33 individuals used different geographical areas and displayed frequent dives to shallow
34 depths (10-30 m). All fish that entered the Labrador Sea (n = 8) migrated through the
35 Strait of Belle Isle (767 km from the river mouth), after spending 41-60 days in the
36 Gulf of St. Lawrence. After exiting the Gulf of St. Lawrence, individuals utilized
37 different areas in the Labrador Sea, and overlaps in spatial distributions among the
38 individuals were largely limited to the Labrador Coast. This variation in area use was
39 accompanied by individual differences in diving behaviour, with maximum depths
40 recorded for individuals ranging from 32 to 909 m. Dives to depths exceeding 150 m
41 were only performed by four individuals and mainly restricted to the central Labrador
42 Sea (areas with water depths > 1000 m). Vertical movements were shallower and
43 resembled those in the Gulf of St. Lawrence when fish migrated through shallower
44 coastal areas along the Labrador Shelf. In conclusion, the large overall variation in
45 migration routes suggests that post-spawners from the Miramichi River encounter
46 different habitats during their ocean migration and that the growth and survival of

47 adults may depend on ecological conditions in multiple regions, both in the Gulf of
48 St. Lawrence and in the Labrador Sea.

49

50 **Introduction**

51

52 Comprehensive descriptions of the movement and spatial distribution of individuals
53 are essential in order to understand how animals interact with their environment
54 (Hays *et al.* 2016). Studying large-scale marine migration and behaviour of fishes
55 have become possible by the development of electronic tags that store information
56 about the environment experienced by the fish (e.g. Howey-Jordan *et al.*, 2013;
57 Guðjónsson *et al.*, 2015). For pelagic species that migrate over large spatial scales, the
58 most common tag type used for describing migration is the pop-up satellite archival
59 tag (PSAT, e.g. Block *et al.*, 2011). These tags are attached externally to the animals
60 before they detach after a pre-programmed time period, surface, and transmit archived
61 data and their current position to the Argos satellite system. The use of PSATs has
62 facilitated great advances in examining the ocean distribution and migratory
63 behaviour for pelagic fishes, providing indispensable information for management
64 and conservation (e.g. Lacroix, 2013; Lea *et al.*, 2015)

65

66 For Atlantic salmon (*Salmo salar* L.), the number of large-scale studies of their ocean
67 migration is increasing (Chittenden *et al.*, 2013; Lacroix, 2013; Guðjónsson *et al.*,
68 2015). Nonetheless, most knowledge regarding the marine distribution of Atlantic
69 salmon still originates from conventional tagging studies based on reports of
70 recaptures in fisheries (Dadswell *et al.* 2010, Jacobsen *et al.* 2012, Reddin *et al.*
71 2012). Studies based on reported recaptures provide invaluable information about the

72 general distribution patterns of stock complexes, but fail to describe accurate space
73 use and behaviour both on individual and population level, and are biased towards
74 areas where fisheries have taken place. As a result, detailed knowledge of movement
75 at sea is still required for many populations, particularly in light of the species'
76 current conservation status (Hansen *et al.* 2012).

77

78 During the past decades, substantial declines in population sizes have been observed
79 for numerous populations of Atlantic salmon, particularly in the southern part of the
80 distribution range where many are currently on the brink of extinction (Chaput 2012,
81 ICES 2015). On local and regional scales, the causal mechanisms behind the declines
82 are diverse and include: parasite induced mortality from salmon lice infestation (e.g.
83 Gargan *et al.*, 2012; Krkosek *et al.*, 2013), introduced parasites (e.g. Harris *et al.*,
84 2011), genetic introgression from farmed Atlantic salmon (e.g., Glover *et al.*, 2013),
85 degeneration of freshwater habitats (Parrish *et al.*, 1998; Otero *et al.*, 2011), and
86 overharvesting (e.g. Parrish *et al.*, 1998). On a broad scale, changes in marine
87 ecosystems are considered prominent contributors to the recent declines, as
88 decreasing return rates often correlate with increases in sea surface temperatures
89 (Friedland *et al.*, 2009a; Otero *et al.*, 2011; Chaput, 2012). For European populations,
90 it is perceived that these temperature induced population declines are associated with
91 shifts in marine food web structure that reduce post-smolt growth during the first
92 months at sea (McCarthy *et al.*, 2008; Friedland *et al.*, 2009a). This differs, at least in
93 parts, compared to populations from the Northwest Atlantic where population
94 declines can be linked to both temperature induced reduction on individual growth
95 (Mills *et al.* 2013, Renkawitz *et al.* 2015), and/or changes in predator fields (Friedland

96 *et al.* 2009b, 2012). Nevertheless, more information about the large-scale ocean
97 distribution and migration routes of Atlantic salmon is needed.

98

99 To date, individual migration routes for North American Atlantic salmon have been
100 addressed in only one published study, where the migratory behaviour of post-
101 spawned adults, tagged with PSATs in the Bay of Fundy, varied among populations
102 with the longest recorded migration terminating at the Labrador Coast (Lacroix 2013).
103 Although studies on the migration of post-spawners do not address the most critical
104 life stage (i.e. post-smolts), these studies are of great importance because post-smolts
105 and previous-spawned Atlantic salmon show some overlap in marine distribution
106 (Sheehan *et al.* 2012, Renkawitz *et al.* 2015), and repeat spawners play an important
107 role in maintaining recruitment particularly in years with low post-smolt survival
108 (Halttunen 2011). Consequently, novel information about the migration of post-
109 spawned individuals is essential in developing a greater understanding of how
110 Atlantic salmon interact with their environment – and of the ongoing process that has
111 left a vast number of stocks at peril.

112

113 The Miramichi River, Canada, supports the largest Atlantic salmon population in
114 North America. In recent decades the spawning stock in the river has collapsed
115 despite monumental reduction in fishing pressure (Friedland *et al.*, 2009b; Chaput and
116 Benoît, 2012). Here, we present a detailed analysis of the marine migration and
117 behaviour of post-spawned Atlantic salmon from the Miramichi River, concurrently
118 tagged with PSATs and acoustic transmitters. The combination of satellite and
119 acoustic telemetry has previously been use for describing coastal movement in other
120 salmonids (Teo *et al.* 2013), but the current study is the first to utilize both

121 technologies in describing the large-scale oceanic migration of Atlantic salmon. Our
122 primary aim was to reconstruct the movement of individual post-spawners using a
123 Hidden Markov Model (HMM), which predicts the probability of individuals
124 occupying different geographic positions on a daily basis and reconstructs movement
125 tracks using data retrieved from individual tags (Thygesen *et al.*, 2009; Pedersen,
126 2010). We also investigated vertical profiles in relation to diel periods and spatial
127 distribution in addition to temperature ranges experienced by the fish during the
128 marine migration.

129

130 **Material and Methods**

131

132 Study area

133

134 The Miramichi River is located within the western Gulf of St. Lawrence (47.2°N, -
135 65.0°W) and drains an area of approximately 12,000 km² (Figure 1). It is divided in
136 two main branches, the Southwest Miramichi and the Northwest Miramichi, which
137 join in the estuary before the river terminates in the Miramichi Bay. Over a four-year
138 period, starting in 2012, post-spawned adult Atlantic salmon (kelts) were tagged with
139 PSATs and acoustic transmitters. Kelts were caught in the Northwest Miramichi
140 River by fly-fishing from 20 April to 16 May each year and brought to shore in live
141 wells for tagging. All tagged kelts were at least 70 cm in length to accommodate the
142 size of the tags. A total of 43 kelts were tagged (42 females, 1 male), with a mean
143 total length of 78 cm (range 70-93 cm, SD ± 5 cm) and average mass of 3.5 kg (range
144 2.3-6.1 kg, SD ± 0.8 kg).

145

146 Tagging procedure

147

148 The fish were anaesthetized using clove oil (Hilltech Canada, Canada) at a
149 concentration of 40 mg/l river water. During surgery, the fish were provided with a
150 flow of fresh river water over their gills. Kelts were first fitted with an acoustic
151 transmitters that was inserted into the body cavity through a 15 mm incision made
152 slightly lateral to the mid-ventral line approximately 20 mm anterior to the pelvic fins.
153 Two sutures (nylon, size 2-0, Ethicon Inc., Pennsylvania, USA) were used to close the
154 incision.

155

156 Next, a PSAT was attached using a similar method to that described in Courtney et al.
157 2016. First, the tags were attached to two 50 mm long cushioned rigid back plates
158 using a nylon braid. The back plates were then wired through the dorsal musculature
159 below the dorsal fin using two biocompatible plastic coated stainless steel wires. A
160 part of the braid attaching the PSAT to the harness was encapsulated in plastic coating
161 to lift the PSAT up from the back of the fish, reducing the chances of skin wounds
162 from the tag scratching on the skin of the fish. This made the tag lie 1-2 cm above and
163 behind the dorsal fin minimizing drag and buoyancy (Supplementary figure 1). A
164 biocompatible silicon pad was glued on the inside of the plates to reduce abrasion on
165 the skin and a small plastic tag (Floy Tag Inc., Washington, USA) was attached to one
166 of the plastic plates with contact information for anglers in the event of recapture. The
167 entire process to insert an acoustic transmitter and attach a PSAT lasted 4-5 minutes.

168

169 After tagging, fish were placed in holding boxes in the river and monitored for a
170 minimum of one hour after tagging. Fish were upright between four and six minutes

171 after PSAT attachment, and reacted to external stimuli shortly afterwards. No
172 excessive bleeding was recorded. Once recovered, the fish were released into the river
173 at the surgery site (n = 32) or, in 2014, placed in oxygenated tanks and trucked 2 km
174 downstream to bypass large numbers of anglers in the tagging area (n = 11). The
175 tagging was approved under licence by Department of Fisheries and Oceans Canada
176 (license numbers SG-NBT-12-032A, SG-RHQ-13-036A, SG-RHQ-14-021, SG-RHQ-15-
177 005).

178

179 Tag and tracking details

180

181 The PSATs used in this study were X-tags (12 × 3.2 cm, 40 g in air) manufactured by
182 Microwave Telemetry, Columbia, Maryland. These tags record temperature, depth,
183 and light intensity at two-minute intervals, and calculated a daily geolocation based
184 on sunrise and sunset estimates for up to 16 months. The daily latitudes are calculated
185 using the estimated day lengths, whereas longitudes are calculated by dusk-dawn
186 symmetries. Similar to all other methods for geolocation based on light levels, this
187 approach provides more accurate estimates of longitude than latitude, particularly in
188 periods around the equinoxes (Hill and Braun 2001, Musyl *et al.* 2001).

189

190 Tags were programmed to release on 31 August, 30 September, and 31 October in the
191 year of tagging, with deployment periods between 114 and 177 days. A failsafe
192 release was also programmed to account for situations when pressure (depth) was
193 constant (corresponding to a 2 m depth band) for more than 4-5 days, or if the fish
194 dived to depths endangering the physical integrity of the tag (manufacturer specified
195 at 1250 m). In addition, the tags were programmed to not detach during the first 22 to

196 25 days after tagging (22 days in 2012, 2013 and 25 days in 2014, 2015). This
197 prevented detachment if the tagged fish remained at constant depths in the river.
198 Temporal resolution of the data retrieved from X-tags depends on the deployment
199 duration and whether or not the tags are physically retrieved. Tag recovery allows
200 access to the full data set, whereas for non-recovered tags only a subset of the time
201 series is accessible depending on the amount of data successfully transmitted to the
202 satellites. A completely transmitted data set would include: daily geolocation
203 estimates, daily sunrise and sunset estimates, daily summaries of temperature and
204 depth, 15-min interval recordings of depth and temperature for the first 4 months of
205 deployment, and 30-min interval recordings for the days after this threshold. Notably,
206 for non-recovered X-tags, compression techniques implemented in the tags may cause
207 reporting of delta-limited values
208 (http://www.microwavetelemetry.com/fish/understanding_data_xtag.cfm). If present,
209 these values represent distorted measurements of depth and temperature, and they
210 occur when the changes exceeds a certain threshold. This causes underestimation of
211 the true values during drastic increase in depth or temperature and overestimation of
212 true values during drastic decrease in the same variables.

213

214 For the acoustic tracking, we used V9 transmitters (29 mm × 9 mm, VEMCO,
215 Halifax, NS, Canada), which emit signals at 69 kHz and have a lifespan of 272 days.
216 VEMCO VR2W and VR4 receivers were strategically deployed at positions covering
217 the entry and exit points of the Gulf of St. Lawrence (Figure 1). This was done to
218 increase the number of known position independent of the PSAT data, and decrease
219 the uncertainty of the geolocation model. Acoustic receivers were deployed near the
220 river mouth (n = 6), at the Miramichi Bay exit to the Gulf of St. Lawrence (n = 11)

221 and at the two main exits from the Gulf of St. Lawrence, which were i) Strait of Belle
222 Isle, between Newfoundland and Labrador (n = 23), and ii) the Cabot Strait, between
223 Newfoundland and Cape Breton Island (n = 162) (Figure 1). Receivers at the Cabot
224 Strait constitute the Cabot Strait Line, operated by the Ocean Tracking Network,
225 Dalhousie University, Halifax, NS, Canada (Castonguay *et al.* 2009). In 2015, a
226 second Strait of Belle Isle transect of receivers (n = 28) was deployed approximately
227 3.5 km northeast of the first gate to increase the likelihood of detecting tagged fish.
228 All receivers were seasonal (deployed in spring and removed by fall), with the
229 exception of the Cabot Strait line, which operates year round. The spacing distance
230 between receivers in transects (Miramichi Bay, Strait of Belle Isle and Cabot Strait)
231 was maximum 800 m, which is considered to provide complete detection coverage for
232 V9 tags under ideal conditions.

233

234 Migration model

235

236 We modelled the movement of tagged Atlantic salmon using a discrete-time Hidden
237 Markov Model (HMM), developed for geolocating fish (Thygesen *et al.*, 2009;
238 Pedersen, 2010). HMMs are state-space models in which location distributions are
239 non-parametric and enable reconstruction of movement in non-linear environments,
240 while accounting for the uncertainty of the data (Pedersen 2010). The non-parametric
241 nature of the location distributions differ compared to Kalman filter techniques (e.g.
242 Sibert *et al.*, 2003; Nielsen *et al.*, 2006), which despite being highly efficient in
243 describing migration over open waters, often assign non-zero probabilities to
244 positions on land in non-linear environment (Pedersen 2010). We chose the HMM
245 framework because the tagged fish encountered areas with complex boundaries

246 between land and ocean during large parts of their marine migration. Furthermore,
247 since the quality of input data from the PSATs were occasionally compromised by the
248 mode of transmission, we wanted to use a model that explicitly accounted for this
249 uncertainty. In the following section, we describe our specific model, which could be
250 replicated and improved in further studies. For the mathematical theory and
251 assumptions behind geolocation using HMMs, we refer to Pedersen (2010). All model
252 implementations were conducted in the R environment (R Core Team 2015).

253

254 In HMMs, the posterior distribution at each discrete time step is estimated by a two-
255 step forward running Bayesian filter, followed by a backward smoothing step refining
256 marginal distributions conditional on all data (Pedersen 2010). In the forward filter,
257 non-parametric posterior distributions are calculated by coupling of two stochastic
258 models: the process model (i.e. time update), which represents the movement scheme
259 and predicts the underlying evolution of probability densities; and the observational
260 model (i.e. data update) that refines these probability densities depending on the data
261 (Thygesen *et al.*, 2009; Pedersen, 2010).

262

263 HMMs rely on discretization of time and space, allowing posterior distributions to be
264 estimated by a numerical solution of the underlying movement process. We used
265 time-step length of one day, meaning that positional probabilities were estimated on a
266 daily basis. For the process model we assumed fish to move according to a diffusion
267 process, given by the diffusion equation (Codling *et al.* 2008).

268

$$269 \quad \partial\phi(\mathbf{x},t)/\partial t = D\nabla^2\phi(\mathbf{x},t) \tag{1}$$

270

271 where $\phi(\mathbf{x},t)$ is the probability that a fish is present at location \mathbf{x} at time t , ∇ is the
272 spatial gradient operator, and D represents the diffusivity parameter. Here, movement
273 probabilities between days were constructed by solving equation (1) using the finite
274 difference method (see Thygesen *et al.*, 2009 for solution) on the discretized grid
275 multiple times for each time step. This was done in order to implement more realistic
276 movement between days, allowing individuals to perform multiple short movements
277 in a single day (Supplementary figure 2). For our final solution, we used an
278 equidistant grid of 10 km in each direction at ten recursive solutions allowing
279 individuals to move a maximum daily distance of 100 km. Movement onto land was
280 prevented by setting transition probabilities onshore to zero. In order to avoid loss of
281 probability mass the remaining transition probabilities were then normalized.

282

283 Daily likelihoods of each position in the grid were constructed using filtered daily
284 geolocation estimates (i.e. latitude and longitude), daily mean temperature of PSAT
285 recordings at the surface (>5m), and daily maximum depth. The raw geolocation
286 estimates reported by the tags were filtered as follows: first, a subjective removal was
287 conducted omitting days when time of sunrise and/or sunset were measured at depths
288 exceeding 10 m. This threshold depth was chosen, as this was the only depth bin
289 running from the surface with 10 m increments where less than 5 % of light values
290 were influenced by vertical movements for all recovered tags with available light
291 data. Second, an objective removal was implemented. Here, a generalized additive
292 model (GAM) with day length as the dependent variable and Julian days as a
293 smoother was fitted, rejecting days with residuals exceeding a set threshold ($2 \times$
294 residual standard deviation). Smoothing parameters of regression curves were
295 selected using generalized cross validation. Latitude estimates 14 days prior and after

296 the autumn equinox were omitted, as this period produces unreliable latitude
297 estimates as day lengths are approximately equal across all latitudes (Hill and Braun
298 2001, Musyl *et al.* 2001). In estimating longitude, the equinox problem is negligible
299 as they rely on the dusk and dawn symmetry, and measurement error is constant
300 throughout the year (Hill and Braun 2001). Likelihood fields for the filtered raw
301 geolocations were calculated assuming independent Gaussian distributions for latitude
302 and longitude, using the filtered estimates as means. Standard deviation in longitudes
303 was fixed to 0.5° , whereas for latitude the standard deviation was set to 1.5° for days
304 with appropriate distance from the autumn equinox. These parameters were selected
305 based on the expected uncertainties given by Microwave Telemetry for the X-tag used
306 at latitudes between 65°S and 65°N , and the general variability of geolocation
307 estimates by PSATs (Musyl *et al.* 2001).

308

309 Daily temperature observations at each position were modelled as Gaussian random
310 variables, with daily observed values and measurement errors derived from the
311 Operational Sea Surface Temperature and Sea Ice Analysis (OSTIA) database at that
312 respective positions as the means and standard deviations (http://ghrsst-pp.metoffice.com/pages/latest_analysis/ostia.html). For the depth filter, a rejection
313 algorithm was implemented, setting data likelihoods to zero if maximum depth
314 recorded by the tag exceeded the bathymetry at that position, and to one otherwise
315 (http://www.gebco.net/data_and_products/gridded_bathymetry_data/). The posterior
316 distributions of the time and data update, $\phi(\mathbf{x}, t)$, were then calculated:

318

319
$$\phi(\mathbf{x},t) = \frac{\phi(\mathbf{x},t-1) * TP * L(\mathbf{x},t)}{\lambda(t)} \quad (2)$$

320

321 where $\lambda(t)$ denotes the normalization constant, $\phi(\mathbf{x},t-1)$ is the posterior distribution the
322 previous day, TP is the convolution scheme (Supplementary figure 2) and $L(\mathbf{x},t)$ is the
323 product of the different likelihood fields.

324

325 The diffusivity parameter, D, was fixed to the highest possible value that prevented
326 numerical oscillations and ensured that all probabilities were positive (i.e. stability
327 criterion of the finite difference method). In order to filter the posterior distributions
328 conditional on all data in the time series, the backward smoothing described in
329 previous geolocation papers using HMM was applied (e.g. Thygesen *et al.* 2009,
330 Pedersen 2010). Individuals' most likely movement paths were estimated using the
331 Viterbi algorithm (Viterbi 2006) and overall space use was quantified by the overall
332 residency distribution (Pedersen *et al.* 2011). The overall residency distribution, RD,
333 is a cumulative distribution representing the expected amount of time an individual
334 uses at all positions in the spatial domain, thus accounting for the spatial uncertainty
335 in the estimates (Pedersen *et al.* 2011).

336

337 Vertical movement

338

339 For individual fish, diel differences in depth distributions and vertical displacements
340 were investigated independently during occupancy of different oceanographic regions
341 using one-way permutation tests (i.e. randomisation tests). The defined regions were
342 the Gulf of St. Lawrence, and coastal and non-coastal waters in other areas. The

343 division of the time series was based on the most likely movement path of individual
344 fish. Segregation of waters outside the Gulf of St. Lawrence depended on whether the
345 fish migrated over coastal shelves or non-coastal waters, categorized by a depth
346 threshold of 1000 m, for consecutive days. This was implemented to prevent
347 excessive partitioning of periods when fish migrated close to coastal shelves. Diel
348 periods were determined by civil sunrise and sunset, which correspond to 30 min
349 before sunrise and 30 min after sunset. For days with unreliable estimates, sunrise and
350 sunset data were generated by linear interpolation.

351

352 **Results**

353

354 *Fate of tagged fish and data recovery*

355

356 Data from the marine migration were retrieved from 24 PSATs, whereas 4 tags were
357 expelled prior to ocean entry and 15 PSATs did not transmit data for unknown
358 reasons. The tags with successful data retrieval were i) successful detachments at
359 programmed pop-up date (n = 6), ii) premature pop-ups after ocean entry (n = 16: 7
360 reporting for unknown reasons and 9 with temperature and depth profiles associated
361 with ingestion by marine predator), or iii) retrieved from fish returning to the river as
362 consecutive spawners in the same year as they were tagged (n = 2).

363

364 Of the 24 fish tagged with reporting PSATs, 22 were detected by the acoustic
365 receivers when leaving the river, 3 fish were recorded by acoustic receivers when
366 passing the Strait of Belle Isle and none were recorded leaving the Gulf of St.
367 Lawrence via the Cabot Strait. For the fish tagged with non-reporting PSATs, 13 of

368 15 individuals were detected leaving the river and 6 were detected passing the Strait
369 of Belle Isle. Hereafter, only data from fish tagged with reporting PSATs are
370 described. The median time spent in the river after tagging was 14 days (range = 6-42
371 d, $SD \pm 10$ d), with individuals entering the sea between 2 May and 7 June. For the
372 three fish that were detected by acoustic receivers when passing the Strait of Belle
373 Isle, residency times in the Gulf of St. Lawrence were 41, 45, and 51 days. The two
374 consecutive spawners spent 70 and 38 days reconditioning in the Gulf of St.
375 Lawrence before returning to the river.

376

377 Quantity of transmitted data varied between tags, largely dependent on the fate of the
378 fish and pre-programmed pop-up date, with the total number of logged days ranging
379 from 7 to 141. Only fish that spent more than 30 days at sea had their migration
380 reconstructed ($n = 16$: 6 reaching the due date, 7 with temperature and depth profiles
381 associated with predation, 1 surfacing prematurely after a period on the ocean floor,
382 and 2 fish returning to the river in the same year as tagging). For these fish, 4 tags
383 were physically retrieved, whereas data from 12 tags were recovered from satellites
384 (range = 43 – 100 %).

385

386 The start points of the HMM were set as individuals' last acoustic fix in the estuary or
387 bay, or by investigating the tags temperature profile if fish were not acoustically
388 detected entering the Gulf of St. Lawrence. For the tags reporting as scheduled and
389 for the tag dwelling on the ocean floor, end points were set as the first reported Argos
390 position and treated as certain in the HMM. This was a reasonable assumption for the
391 sinking tag, as depth recordings prior to surfacing were constant and corresponded
392 with the bathymetry at the surfacing position. For tags with temperature and depth

393 profiles corresponding with ingestion by a predator, end points were not fixed and
394 candidate positions were represented by their probability at the day of predation along
395 a time series including the post-predation period. For individuals recorded passing the
396 acoustic gates at the Strait of Belle Isle, acoustic fixes were treated as certain.

397

398 Horizontal movement

399

400 For the tracked individuals, end points of migrations were in the Labrador Sea for
401 eight fish, whereas the remaining tracks ended in the Gulf of St Lawrence (Figure 2
402 and 3). For all tracked individuals, the overall and daily residency distributions were
403 densely centred, with most of the probability mass occupying a small spatial region
404 throughout the migrations (Supplementary figure 3; Supplementary video 1 and 2).
405 For the three fish that were detected by acoustic receivers when passing the Strait of
406 Belle Isle (straight line distance of 767 km from river mouth) the estimated timing of
407 passage, calculated by running the HMM ignoring the acoustic detection, were
408 identical to the actual passage times (41, 45, and 51 days after leaving the river). This
409 confirms the reliability of the HMM.

410

411 The most likely tracks for the geolocated fish that entered the Labrador Sea without
412 being detected by acoustic receivers ($n = 5$) indicated that these fish also passed
413 through the Strait of Belle Isle, after an estimated median residency time in the Gulf
414 of St. Lawrence of 44 days (range = 42-60 d, $SD \pm 7$ d). For all fish that migrated
415 through the Strait of Belle Isle, passage dates were between 27 June and 12 July ($n =$
416 8).

417

418 During the residency in the Gulf of St. Lawrence, individuals utilized different areas
419 shortly after ocean entry. The most likely tracks and daily residency distributions
420 indicated overall utilization of areas spanning from waters adjacent to Prince Edward
421 Island towards waters north of Anticosti Island (Figure 2 and 3; Supplementary figure
422 3). For fish entering the Labrador Sea, average migration speeds from the river mouth
423 to the Strait of Belle Isle ranged from 19.4 – 26.1 km/d ($n = 8$, median = 23.9 km/d,
424 $SD = \pm 2.3$ km/d), based on the most likely movement paths.

425

426 For individuals passing the Strait of Belle Isle ($n = 8$), tags logged for 18-94 days
427 after entering the Labrador Sea, with most likely movement paths and residency
428 distributions of individuals spanning from coastal waters of Newfoundland, towards
429 Baffin Bay and the west coast of Greenland (Figure 2; Supplementary figure 3).
430 Despite large variation in individual movement paths after exiting the Gulf of St.
431 Lawrence five individuals displayed similar migratory trajectories during initial
432 residency in the Labrador Sea, with persistent migration northwards along the
433 Labrador Coast. For the remaining fish ($n = 3$), two individuals migrated towards
434 deeper waters in the central Labrador Sea shortly after strait passage, whereas one fish
435 resided in areas of the coast of Newfoundland for an extended period before migrating
436 to the central Labrador Sea (Figure 2). Notably, neither of the similarities in migratory
437 behaviours remained consistent throughout the occupancy of the Labrador Sea, with
438 further diversification during the periods leading up to tag detachments (Figure 2).
439 The most distant location from the Strait of Belle Isle for these individuals was
440 median 1070 km ($n = 8$, range = 404 – 1590 km, $SD \pm 416$ km), and average
441 individual migration speeds after passing the strait ranged from 17 – 35.8 km/d
442 (median = 28.3 km/d, $SD \pm 5.2$ km/d), based on the most likely migration routes.

443

444 Vertical movement and temperature range

445

446 Individuals were generally associated with surface waters during their marine
447 migration, with all fish spending more than 67% of the time in the upper 10 m of the
448 water column (Figure 4). Maximum depths recorded by the 16 tags ranged from 38-
449 909 m (median = 97 m, SD \pm 331 m). Only four fish performed deep dives exceeding
450 150 m. The overall temperature experienced by the fish ranged from -1.3°C to
451 17.9°C, with all recordings below 0°C occurring during vertical movements in
452 stratified waters.

453

454 Within the Gulf of St. Lawrence, all fish exhibited frequent vertical movements to
455 various depths in the upper 50 m of the water column (Figure 2 and 3). Dives
456 exceeding 30 m were rare, and maximum depths within the Gulf of St. Lawrence
457 were between 38-163 m (median = 83 m, SD \pm 39 m). All fish occupied greater
458 depths and exhibited greater vertical movements during the day than during the night
459 when residing within the Gulf of St. Lawrence (permutation-tests; p-values < 0.025,
460 median depths day = 0.7-7.4 m, median depths night = 0-2.7 m). Water temperatures
461 experienced by the fish during these periods ranged from 0°C to 17.9°C, with
462 individual mean temperature ranging from 6.3°C to 11.1°C.

463

464 After entering the Labrador Sea, maximum depths ranged from 32-909 m (median =
465 362 m, SD \pm 410 m). Here, temperatures experienced by the fish ranged from -1.3°C
466 to 14.9°C, and individual mean temperatures ranged from 4.2°C to 8.5°C. For fish

467 entering the Labrador Sea, mean temperatures were significantly lower than those
468 experienced in the Gulf of St. Lawrence (Wilcoxon signed-rank test; p-value < 0.025).

469

470 For the five fish that migrated northwards along the Labrador Coast after entering the
471 Labrador Sea, all individuals displayed frequent shallow dives, occupied greater
472 depths, and displayed greater vertical movements during the day than night
473 (permutation-test; p-values < 0.025, median depths day 1.3-2 m, median depths night
474 0-1 m). In contrast, for the remaining fish (n = 3), no general trend in diurnal
475 behaviour was present during the initial residency over the coastal shelf of
476 Newfoundland and Labrador (permutation-tests).

477

478 When distributed over waters with depths greater than 1000 m, all fish performed
479 occasional deep dives exceeding 150 m (n = 4, Figure 2). During these periods, only
480 the fish that migrated across the Labrador Sea towards the west coast of Greenland
481 displayed both deeper depth distribution and greater vertical movement during the day
482 (permutation-tests) (Figure 2).

483

484 For the three fish that re-entered coastal waters, residency periods over non-shelf
485 areas lasted for 26, 27, and 31 days. After re-entering shelf waters, all fish (n = 3)
486 performed frequent shallow dives (Figure 2), with one individual utilizing
487 significantly greater depths during the day, and two fish displaying significantly
488 greater vertical displacement in periods of daylight (permutation-tests). The longest
489 residency time over non-shelf waters was 55 days for the fish that remained over deep
490 water until tag detachment.

491

492 **Discussion**

493

494 *Horizontal movement*

495

496 This is the first study to provide detailed descriptions of movement of multiple
497 Atlantic salmon in the Gulf of St. Lawrence and Labrador Sea. Here, we show that
498 individual migration routes diversify immediately after leaving the river, with an
499 escalating degree of spatial diversification for the tagged fish that entered the
500 Labrador Sea through the Strait of Belle Isle. Migrations to the Labrador Sea using
501 the Strait of Belle Isle were expected, as Atlantic salmon from the Miramichi
502 population are known to enter the Labrador Sea via this passage (Ritter 1989).
503 Furthermore, the estimated timing of Gulf of St. Lawrence exit observed in the
504 present study corresponded well with data from conventional tagging studies on
505 previous spawners from the Miramichi River, where most fish were recaptured in
506 proximity to the strait in July (Ritter 1989).

507

508 For Atlantic salmon that migrated to the Labrador Sea, the reconstructed tracks and
509 residency times in the Gulf of St. Lawrence indicate that they were foraging in these
510 areas because both the most likely movement paths and residency distributions show
511 non-directional movements at slow rates. Since the 1990s, the biomass of small fish
512 suitable as Atlantic salmon prey has increased in southern parts of the Gulf of St.
513 Lawrence (Benoît and Swain 2008). This increase in food availability has had a
514 positive effect on consecutive spawners by increasing the proportion of individuals
515 returning to the river after only one summer at sea (Chaput and Jones, 2006; Chaput
516 and Benoît, 2012). In comparison, alternate spawners are seemingly unaffected,

517 indicating a lower overall reliance on the Gulf of St. Lawrence food web for adult
518 Atlantic salmon spending one winter at sea before returning (Chaput and Benoît
519 2012). In context of the present study, it is therefore likely that the growth of alternate
520 spawners is predominately determined by ecological conditions in the Labrador Sea,
521 and it is possible that the positive effects from increased prey abundance in the Gulf
522 of St. Lawrence are masked by the reduced food availability in these areas (Mills *et*
523 *al.* 2013, Renkawitz *et al.* 2015).

524

525 The Labrador Sea is considered the primary overwintering area for North-American
526 Atlantic salmon populations, and utilization of this region has been documented in
527 both conventional tagging studies (Ritter, 1989; Miller *et al.*, 2012) and pelagic
528 surveys that have targeted Atlantic salmon (Reddin and Short 1991, Sheehan *et al.*
529 2012). Despite this, no detailed information exists on how migratory trajectories vary
530 among individuals when distributed in these areas. We show that individuals
531 differentiate in their area use in the Labrador Sea during summer and autumn, and that
532 their total distribution area covers regions known to be utilized by Atlantic salmon
533 (Miller *et al.* 2012, Sheehan *et al.* 2012). This suggests that the growth and survival of
534 adult Atlantic salmon from the Miramichi River likely depends on foraging conditions
535 in multiple regions of the Labrador Sea, during at least parts of their residency in
536 these waters.

537

538 To what extent the observed distribution patterns are maintained in the winter remains
539 unknown because all fish that entered the Labrador Sea experienced tag detachments
540 before 4 October. It is possible that adult Atlantic salmon show more similarities in
541 their spatial distributions later on in their migration, particularly in areas at the west

542 coast of Greenland, which are known as important areas for both maiden and previous
543 spawned individuals (Renkawitz *et al.* 2015). In our study, only one fish entered these
544 waters, after crossing the Labrador Sea in September, and it is possible that a higher
545 proportion of the surviving fish eventually migrated to these areas.

546

547 For Atlantic salmon in general, it has been suggested that the migration may follow
548 the North-Atlantic Sub-polar gyre (Dadswell *et al.* 2010). This hypothesis is largely
549 based on conventional tagging studies on smolts, and suggests that North-American
550 Atlantic salmon that enter the Labrador Sea eventually join the south-flowing
551 Labrador Current (Dadswell *et al.* 2010). In our study, the reconstructed tracks
552 provided no evidence to suggest that migrations follow oceanic currents. Instead,
553 tagged fish that entered the Labrador Sea either displayed migrations against the
554 south-flowing Labrador Current or northwards migrations in the central Labrador Sea.
555 The migratory behaviour displayed by the fish arriving at the west coast of Greenland
556 particularly questions the generality of this hypothesis, as this individual performed
557 counter current migration throughout most parts of its time at liberty. A similar result
558 suggesting that migration of post-spawners is independent of oceanic gyres has
559 previously been recorded for PSAT tagged fish from the Bay of Fundy (Lacroix
560 2013), indicating that horizontal movement of adult Atlantic salmon may be more
561 directly linked to environmental cues governing foraging.

562

563 The overall migration pattern displayed by the post-spawners from the Miramichi
564 strengthens the evidence that Atlantic salmon from North America generally utilize
565 areas farther west in the Atlantic Ocean (Ritter, 1989; Miller *et al.*, 2012) than
566 European populations (Jacobsen *et al.* 2012, Jensen *et al.* 2014). Some European

567 Atlantic salmon are known to migrate to areas along the west coast of Greenland
568 (Hansen and Quinn 1998, Reddin *et al.* 2012, Renkawitz *et al.* 2015), but the
569 Northeast Atlantic Ocean is regarded as their primary destination – with individuals
570 utilizing areas from the Barents Sea to the east coast of Greenland, partially
571 depending on their river of origin (Jacobsen *et al.*, 2012; Jensen *et al.*, 2014). For
572 Atlantic salmon from the Miramichi River, migrations to areas at the Faroe Island
573 have been recorded, indicating that parts of the population utilize areas outside the
574 Labrador Sea (Hansen and Jacobsen 2003). However, in the present study, there was
575 no evidence of trans-Atlantic migrations. This suggests that the spatial overlap
576 between post-spawners from the Miramichi River and individuals from European
577 stocks is limited to areas along the west coast of Greenland. However due to the low
578 sample size and limited duration of the time series, we cannot exclude that some post-
579 spawned individuals migrate to the Northeast Atlantic.

580

581 Vertical movement

582

583 Diving behaviour in Atlantic salmon is generally not well understood, and no study
584 has explicitly addressed the underlying mechanisms of vertical movement. It is likely
585 that diving is driven by foraging, predator avoidance, temperature regulation, and
586 orientation, and that the frequency of dives depends on the stage of migration and the
587 environment that individuals occupy (Reddin *et al.* 2004, 2011, Godfrey *et al.* 2015).
588 Despite this uncertainty, the general consensus regarding continual diving behaviour
589 to shallow depths, typically during the hours of daylight, is that this specific
590 behaviour is associated with foraging in the epipelagic zone (Reddin *et al.*, 2011;
591 Lacroix, 2013). In the present study, this type of behaviour was evident for both

592 consecutive and alternate spawners in the Gulf of St. Lawrence and for alternate
593 spawners when distributed over continental shelves in the Labrador Sea. Given that
594 frequent dives to shallow depth during the day is an appropriate proxy of foraging, the
595 behaviour displayed by the tagged fish is likely to reflect foraging over large
596 geographical areas.

597

598 In the current study, shallow dives and diel effects on vertical movements were
599 mostly absent during periods of deep diving behaviour, and consequently an
600 alternative behavioural mode during these periods can be assumed. The function of
601 deep diving behaviour in Atlantic salmon remains largely speculative, but overall it is
602 likely that they have multiple functions, including foraging, predator avoidance, and
603 searching behaviour. Overall the proportion of fish performing deep dives was low
604 with only 4 of 16 fish analysed showing depth recordings deeper than 150 m. Drag
605 and/or lift caused by the tag may have affected the diving behaviour. In a recent study
606 on Atlantic salmon kelts, Hedger *et al.* (in press) concluded that PSAT tagged fish
607 from European rivers dived less frequently and to shallower depths than individuals
608 tagged internally with small archival tags. Hence, the vertical movements observed
609 here are likely to some extent altered by tagging, but we argue that the observed
610 proportion of fish performing deep dives is likely unaffected, because utilization of
611 depths greater than 150 m was mostly limited to periods of occupancy of waters
612 exceeding 1000 m in depth. This conclusion, supported by the lack of occupancy of
613 depths greater than 50 in a previous tagging experiment on adult North-American
614 using small archival tags (Reddin *et al.* 2011), indicates that deep dives are not
615 performed by all adult Atlantic salmon.

616

617 Geolocation method

618

619 Despite the increasing availability of Hidden Markov models (HMM) to researchers,
620 only one published study has applied this framework for studying the marine
621 migration of Atlantic salmon tagged with archival tags (Guðjónsson *et al.* 2015). For
622 studies aiming to geolocate Atlantic salmon, HMMs could be considered a favourable
623 framework because it can, in addition to estimate migration in coastal areas, also be
624 applied in scenarios without or with poor light-based geolocation estimates (Pedersen
625 *et al.*, 2008; Thygesen *et al.*, 2009; Neilson *et al.*, 2014). Many Atlantic salmon
626 populations migrate to polar areas (Jensen *et al.* 2014), where geolocation from light
627 level algorithms is impossible for large parts of the year, making HMMs applicable
628 throughout the species' distribution range.

629

630 For the daily posterior distributions, the overall uncertainties estimated from our
631 model covered large spatial areas (Supplementary video 1). This was expected, as our
632 model treats uncertainties in a pure sense, creating daily likelihood fields depending
633 on Gaussian random variables without a preset cut-off point. However, it is more
634 important that the centres of the daily probability distributions were dense, indicating
635 high certainty. This is evident by the reduced spatial dispersion of the 95% confidence
636 limits of the daily probabilities (Supplementary video 2), which suggests that the
637 current framework is highly suitable for geolocating Atlantic salmon at these
638 latitudes. This suitability was highlighted by the identical residency times in the Gulf
639 of St. Lawrence when running the model with and without the acoustic detections at
640 the Strait of Belle Isle line for the three fish detected by acoustic receivers when
641 entering the Labrador Sea.

642

643 In comparable studies using HMMs, a directional element in movement is
644 occasionally included by modelling movement as an advection-diffusion process
645 (Pedersen *et al.*, 2011; Neilson *et al.*, 2014). We did not include a directional element
646 in the model, because the persistence of a biased random walk is unlikely in the
647 complex geography that our fish migrated. However, in areas that allow a persistent
648 bias, and where assuming a constant directional preference is reasonable, the fit of
649 both movement schemes should be investigated, because this would potentially
650 decrease the uncertainty of the posterior distributions and reconstructed tracks
651 (Pedersen *et al.* 2011).

652

653 Conclusion

654

655 The present study demonstrates the value of performing long distance tracking studies
656 on pelagic fish using PSATs, as the results show several novel aspects of the marine
657 migration of adult Atlantic salmon. The individual variation displayed throughout the
658 tracking periods suggests that reconditioning success of individual fish likely depends
659 on local ecological conditions, while large spatial areas are important for the
660 population as a whole. This in combination with the spatial differentiation between
661 the North American and European stock complex, add to the consensus that partially
662 different mechanisms are causing the ecosystem driven population declines in the
663 different regions (Friedland *et al.* 2009a, 2009b). Furthermore, we show evidence of
664 consistent diving behaviour during occupancy of different environments, with
665 frequent shallow diving behaviour present along the continental shelf and execution
666 of deeper dives when residing in deeper waters of the Labrador Shelf. This suggests

667 that post-spawned Atlantic salmon display general behavioural modes in different
668 oceanographic environments.

669

670 Supplementary materials

671

672 The following supplementary material is available at ICESJMS online: I)
673 Supplementary figure 1 illustrates the release of an Atlantic salmon tagged with a
674 pop-up satellite archival tag; II) Supplementary figure 2 depicts the convolution
675 scheme of the applied Hidden Markov model, which represents the underlying
676 transition probabilities of the individual movement process from time i to time $i+1$;
677 III) Supplementary figure 3 illustrates the overall residency distributions of the tagged
678 fish that successfully entered the Labrador sea; IV) Supplementary video 1 visualizes
679 the evolution of the daily residency distributions for one Atlantic salmon including
680 the full probability spectra; and V) Supplementary video 2 visualizes the evolution of
681 the daily residency distributions for the same individual with 95 % confidence limit
682 on the daily probabilities (i.e. 95 % of the daily probability mass).

683

684 Acknowledgments

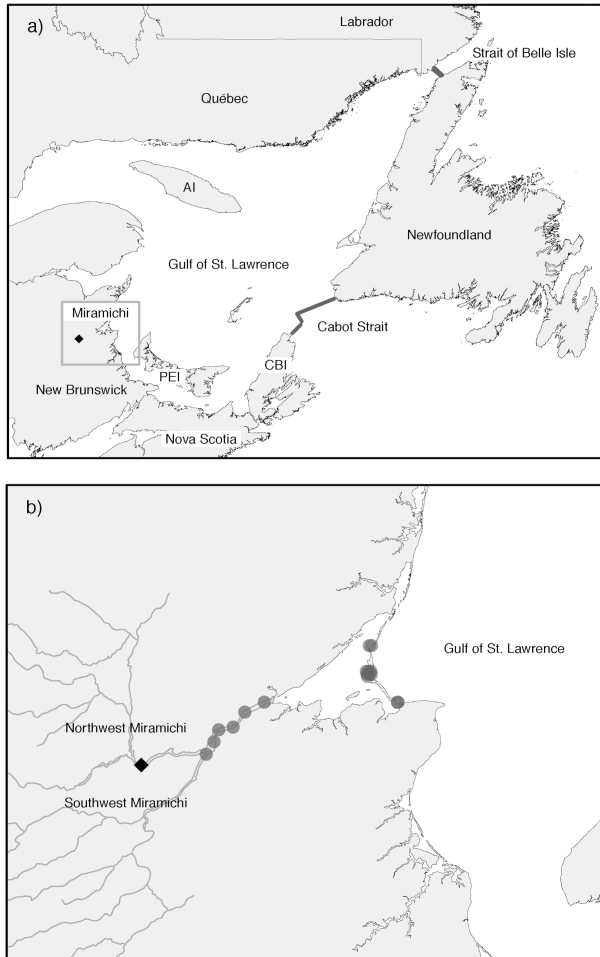
685

686 The authors would like to thank the Miramichi Salmon Association, Mark Hambrook,
687 Holly Labadie, the Atlantic salmon Conservation Foundation, and especially the
688 volunteer anglers and tag sponsors without whom the fieldwork could not have been
689 undertaken. We also thank Serena Wright and Martin W. Pedersen for helpful
690 correspondences regarding the model development, Richard Hedger for generating

691 the spatial grid, and two anonymous reviewers for constructive comments on an
692 earlier draft of the manuscript.

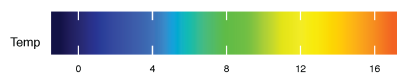
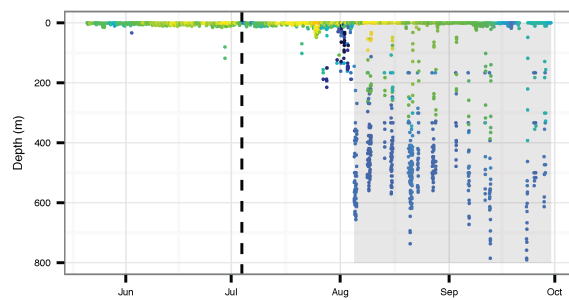
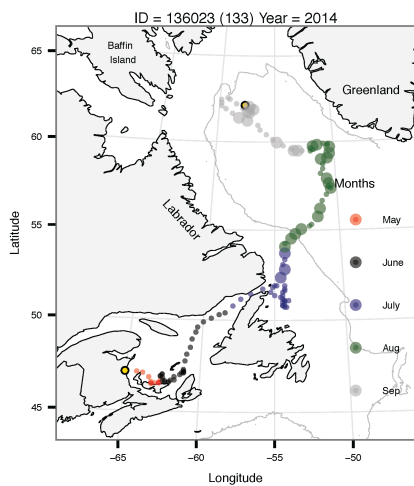
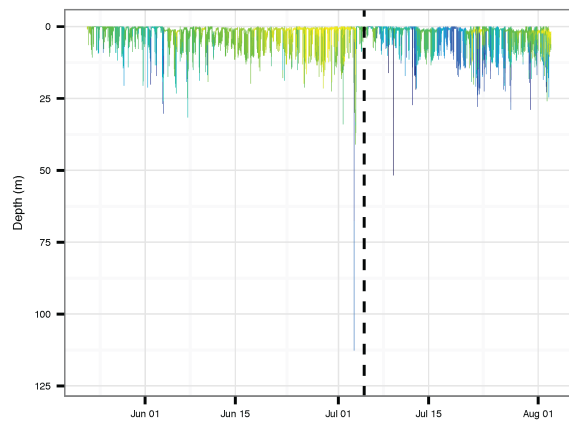
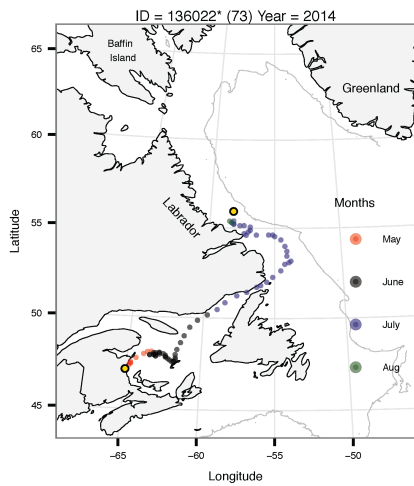
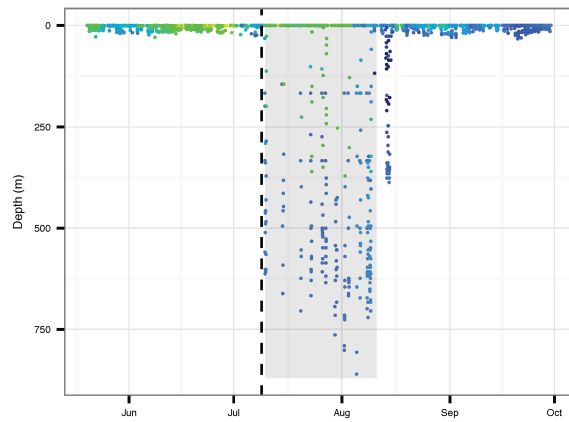
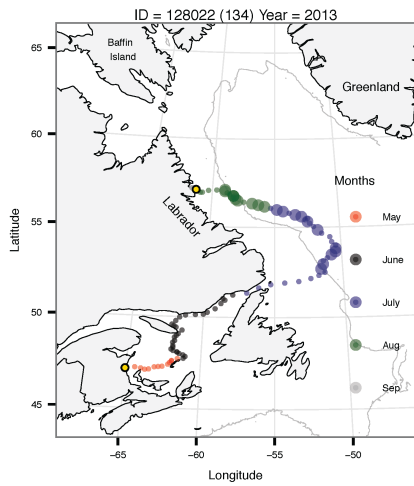
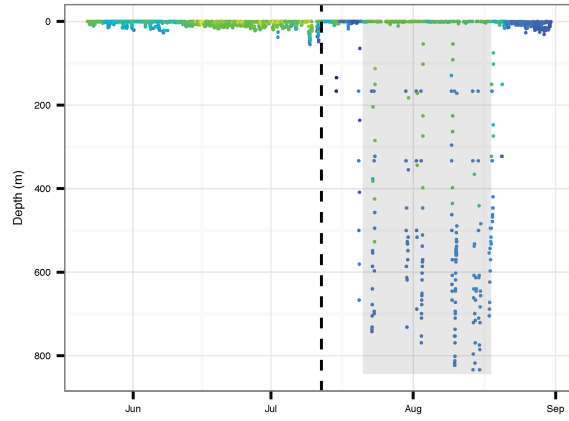
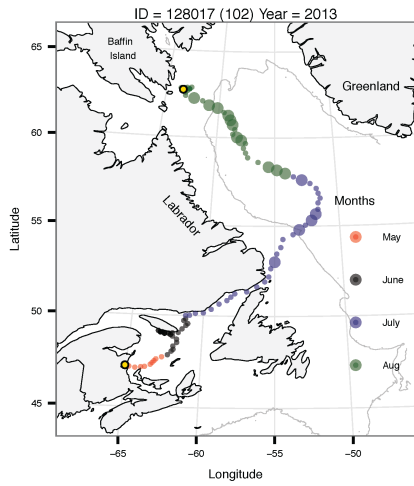
693

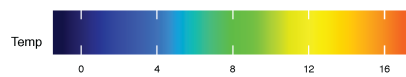
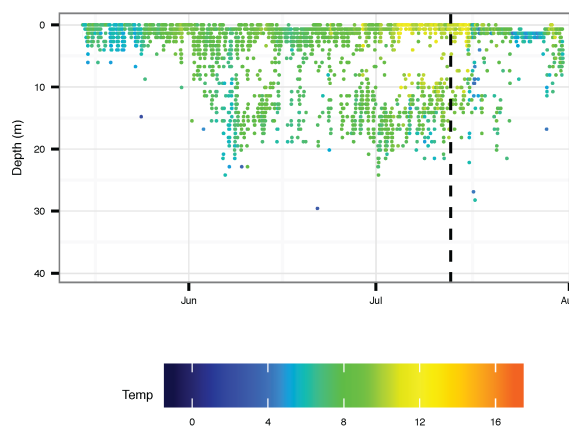
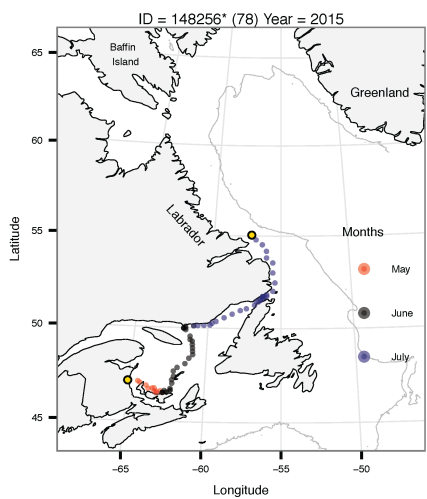
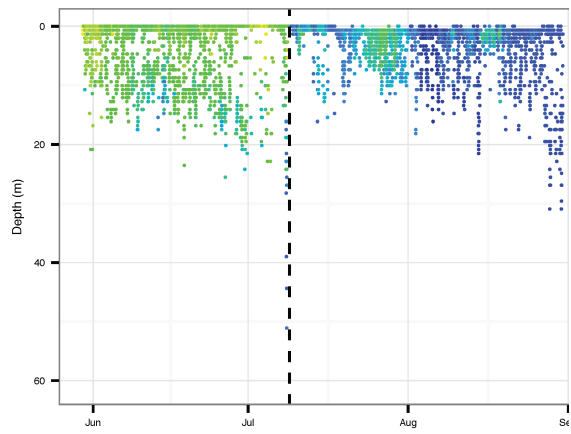
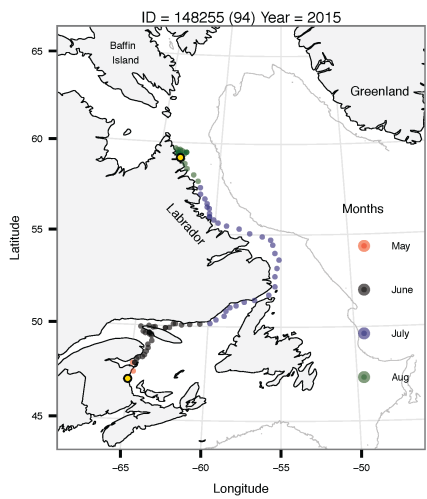
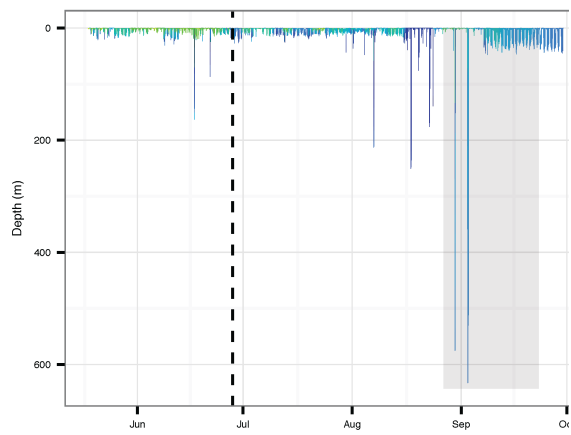
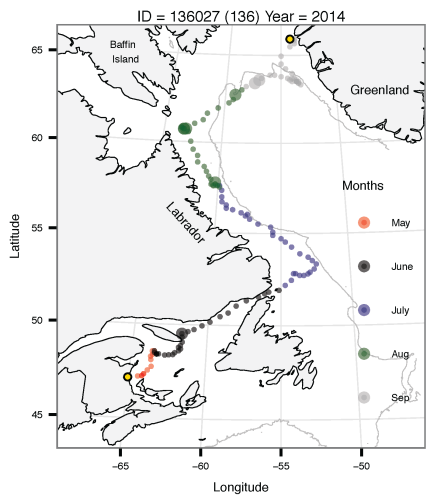
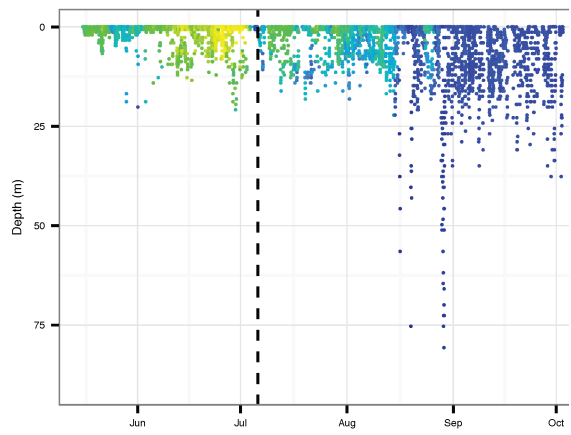
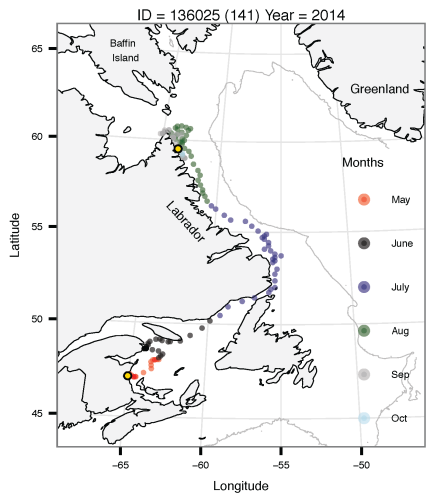
694 **Figures**



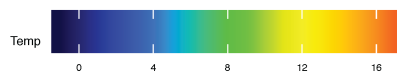
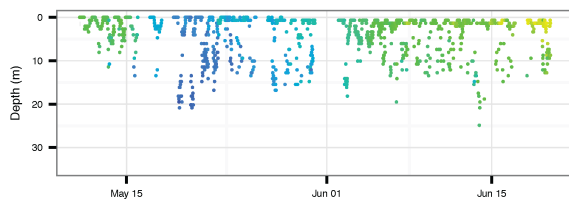
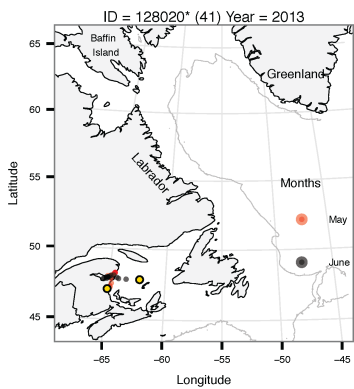
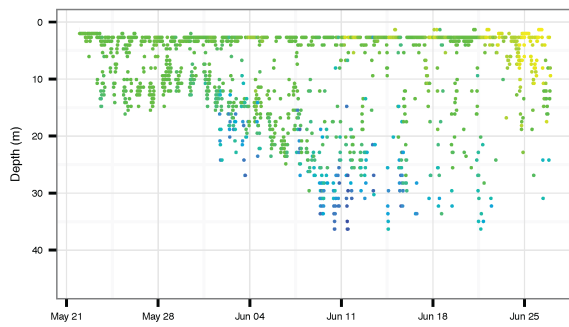
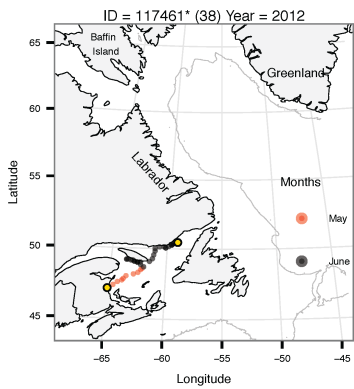
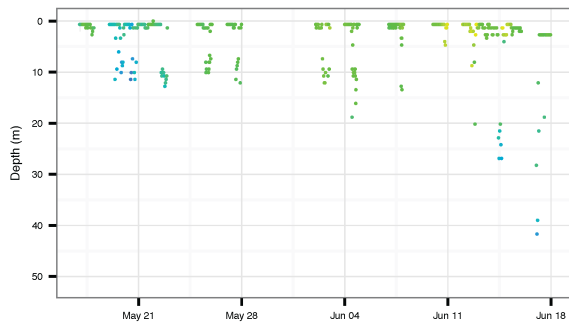
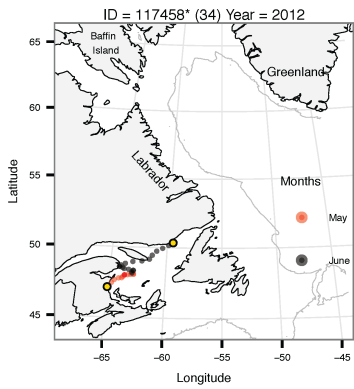
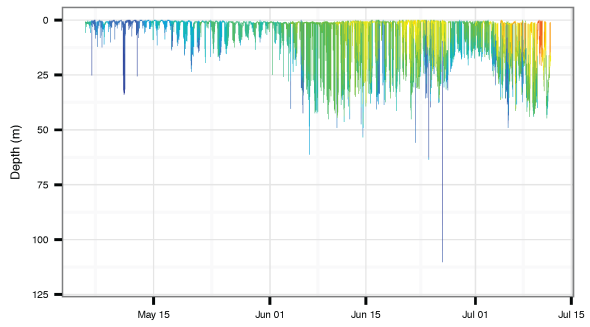
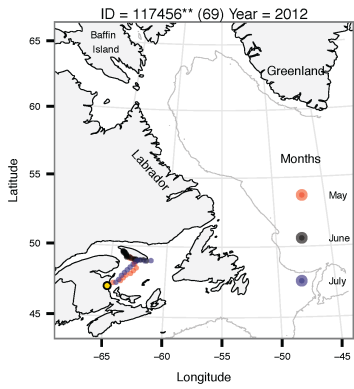
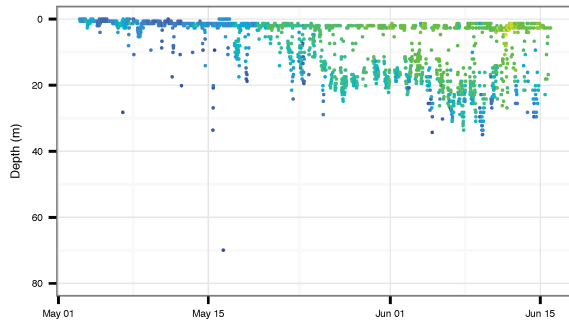
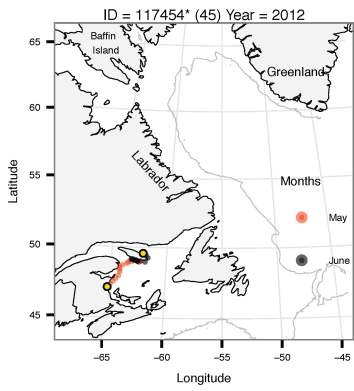
695

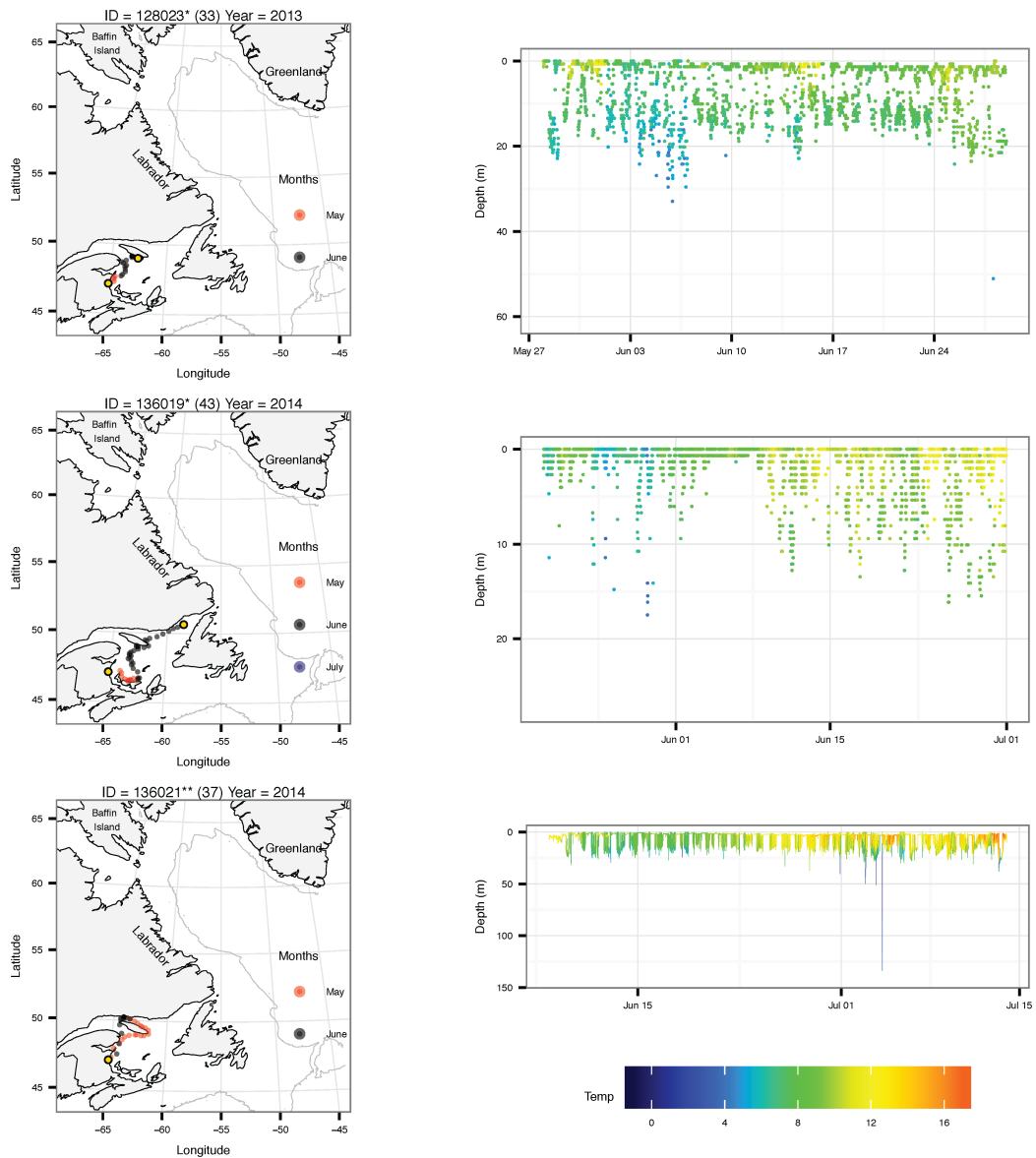
696 Figure 1: Map of study area, including tagging site (black diamond) and acoustic
697 receivers (grey points). Abbreviations listed are: AI = Anticosti Island, CBI = Cape
698 Breton Island, PEI = Prince Edward Island. a) Gulf of St. Lawrence, with acoustic
699 receiver arrays at the Cabot Strait and Strait of Belle Isle (grey box indicates the
700 Miramichi area). b) Miramichi area, including the Miramichi River (grey lines) and
701 acoustic receivers in the river and bay.





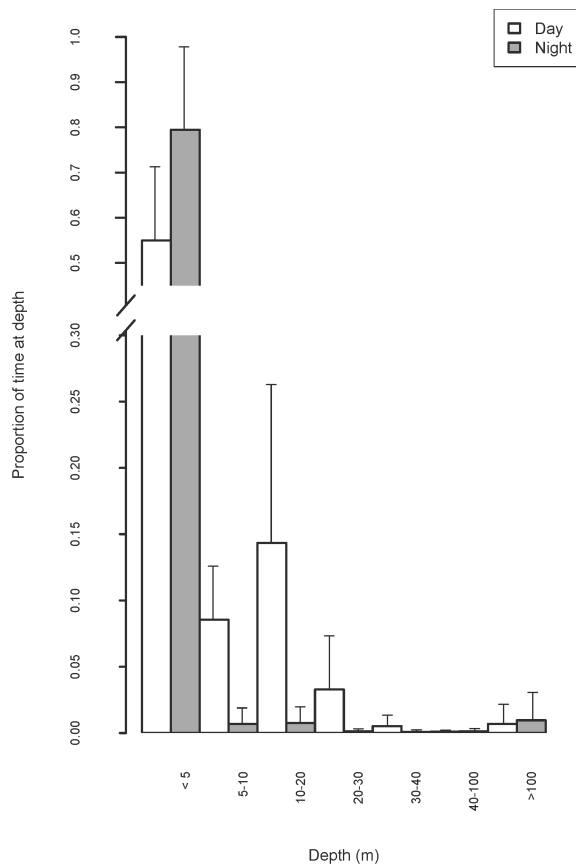
704 Figure 2: Detailed behaviour for the 8 tagged Atlantic salmon that entered the
705 Labrador Sea. Fish experiencing premature tag detachment are noted by *. Left
706 panels: Most likely movement path of individual fish (colour coded by month, yellow
707 circles indicate start and end point of migration, number in parenthesis indicates
708 duration of the marine migration). Large points illustrate days with maximum depths
709 exceeding 150 m, whereas small points indicate days with maximum depths of less
710 than 150 m. Grey line represents the 1000 m bathymetry contour. Right panels:
711 Vertical profiles with corresponding temperatures for the marine migration (illustrated
712 as lines for recovered tags and points for tags that were not retrieved). Colour keys
713 indicate temperatures. Hatched vertical lines demonstrate time of exit from the Gulf
714 of St. Lawrence and shaded areas indicate periods of residency over waters with depth
715 > 1000 m.
716





718

719 Figure 3: Detailed behaviour for the tagged Atlantic salmon that experienced
 720 premature tag detachment in the Gulf of St. Lawrence (n = 6, noted by *) or returned
 721 to the river the same year as tagging (n = 2, noted by **). Left panels: Most likely
 722 movement path of individual fish (colour coded by month, yellow circles indicate
 723 start and end point of migration, number in parenthesis indicates duration of the
 724 marine migration). Grey line represents the 1000 m bathymetry contour. Right panels:
 725 Vertical profiles with corresponding temperatures for the marine migration (illustrated
 726 as lines for recovered tags and points for tags that were not retrieved). Colour keys
 727 indicate temperatures.



728

729 Figure 4: Mean of individuals' mean time spent at different depths during day and
 730 night for the entire marine migration (n = 16). Whiskers indicate standard deviation of
 731 individual means.

732

733 **References:**

734

735 Benoît, H. P., and Swain, D. P. 2008. Impacts of environmental change and direct and
 736 indirect harvesting effects on the dynamics of a marine fish community.

737 Canadian Journal of Fisheries and Aquatic Sciences, 65: 2088–2104.

738 Block, B. A., Jonsen, I. D., Jorgensen, S. J., Winship, A. J., Shaffer, S. A., Bograd, S.

739 J., Hazen, E. L., *et al.* 2011. Tracking apex marine predator movements in a

740 dynamic ocean. *Nature*, 475: 86–90.

741 Castonguay, M., Comeau, L., Swain, D., Bowen, D., O'Dor, R., Stokesbury, M., and
742 Branton, R. 2009. Ocean Tracking Network Cabot Strait line metadata and data
743 set. In O'Dor R., Whoriskey, F., Branton R., and Gross T. 2008 Ocean Tracking
744 Network global equipment deployment and data collection.

745 Chaput, G. 2012. Overview of the status of Atlantic salmon (*Salmo salar*) in the
746 North Atlantic and trends in marine mortality. *ICES Journal of Marine Science*,
747 69: 1538-1548.

748 Chaput, G., and Benoît, H. P. 2012. Evidence for bottom-up trophic effects on return
749 rates to a second spawning for Atlantic salmon (*Salmo salar*) for the Miramichi
750 River, Canada. *ICES Journal of Marine Science*, 69: 1656–1667.

751 Chaput, G., and Jones, R. 2006. Reproductive rates and rebuilding potential for two
752 multi-sea-winter Atlantic salmon (*Salmo salar* L.) stocks of the Maritime
753 provinces. Fisheries and Oceans Canada Canadian Science Advisory Secretariat,
754 Research Document 2006/027. 31 pp.

755 Chittenden, C. M., Fauchald, P., and Rikardsen, A. H. 2013. Important open-ocean
756 areas for northern Atlantic salmon (*Salmo salar*) - as estimated using a simple
757 ambient-temperature approach. *Canadian Journal of Fisheries and Aquatic
758 Sciences*, 70: 101–104.

759 Codling, E. A., Plank, M. J., and Benhamou, S. 2008. Random walk models in
760 biology. *Journal of The Royal Society Interface*, 5: 813–834.

761 Courtney, M.B., Scanlon, B.S., Rikardsen, A.H., and Seitz, A.C. 2016. Utility of pop-
762 up satellite archival tags to study the summer dispersal and habitat occupancy of
763 Dolly Varden in Arctic Alaska. *Arctic*, 69: 137-146

764 Dadswell, M. J., Spares, A. D., Reader, J. M., and Stokesbury, M. J. W. 2010. The

765 North Atlantic subpolar gyre and the marine migration of Atlantic salmon *Salmo*
766 *salar*: the ‘Merry-Go-Round’ hypothesis. *Journal of Fish Biology*, 77: 435–467.

767 Friedland, K. D., MacLean, J. C., Hansen, L. P., Peyronnet, A. J., Karlsson, L.,
768 Reddin, D. G., Ó Maoiléidigh, N., *et al.* 2009a. The recruitment of Atlantic
769 salmon in Europe. *ICES Journal of Marine Science*, 66: 289–304.

770 Friedland, K. D., Manning, J. P., Link, J. S., Gilbert, J. R., Gilbert, A. T., and
771 O’Connell Jr., A. F. 2012. Variation in wind and piscivorous predator fields
772 affecting the survival of Atlantic salmon, *Salmo salar*, in the Gulf of Maine.
773 *Fisheries Management and Ecology*, 19: 22–35.

774 Friedland, K. D., Moore, D., and Hogan, F. 2009b. Retrospective growth analysis of
775 Atlantic salmon (*Salmo salar*) from the Miramichi River, Canada. *Canadian*
776 *Journal of Fisheries and Aquatic Sciences*, 66: 1294–1308.

777 Gargan, P. G., Forde, G., Hazon, N., Russel D.J.F., and Todd, C. D. 2012. Evidence
778 for sea lice-induced marine mortality of Atlantic salmon (*Salmo salar*) in
779 western Ireland from experimental releases of ranched smolts treated with
780 emamectin benzoate. *Canadian Journal of Fisheries and Aquatic Sciences*, 69:
781 343–353.

782 Glover, K. A., Pertoldi, C., Besnier, F., Wennevik, V., Kent, M., and Skaala, Ø. 2013.
783 Atlantic salmon populations invaded by farmed escapees: quantifying genetic
784 introgression with a Bayesian approach and SNPs. *BMC genetics*, 14: 74.

785 Godfrey, J. D., Stewart, D. C., Middlemas, S. J., and Armstrong, J. D. 2015. Depth
786 use and migratory behaviour of homing Atlantic salmon (*Salmo salar*) in
787 Scottish coastal waters. *ICES Journal of Marine Science*, 72: 568–575.

788 Guðjónsson, S., Einarsson, S. M., Jónsson, I. R., and Guðbrandsson, J. 2015. Marine
789 feeding areas and vertical movements of Atlantic salmon (*Salmo salar*) as

790 inferred from recoveries of data storage tags. *Canadian Journal of Fisheries and*
791 *Aquatic Sciences*, 72: 1087-1098.

792 Halttunen, E. 2011. *Staying Alive - The survival and importance of Atlantic salmon*
793 *post-spawners*. Ph.D. thesis, University of Tromsø, Tromsø, Norway. 50 pp.

794 Hansen, L. P., Hutchinson, P., Reddin, D. G., and Windsor, M. L. 2012. *Salmon and*
795 *sea: scientific advances and their implications for management: an introduction*.
796 *ICES Journal of Marine Science*, 69: 1533–1537.

797 Hansen, L. P., and Jacobsen, J. A. 2003. *Origin and migration of wild and escaped*
798 *farmed Atlantic salmon, *Salmo salar* L., in oceanic areas north of the Faroe*
799 *Islands*. *ICES Journal of Marine Science*, 60: 110–119.

800 Hansen, L. P., and Quinn, T. P. 1998. *The marine phase of the Atlantic salmon*
801 *(*Salmo salar*) life cycle, with comparisons to Pacific salmon*. *Canadian Journal*
802 *of Fisheries and Aquatic Sciences*, 55: 104–118.

803 Harris, P. D., Bachmann, L., and Bakke, T. A. 2011. *The parasites and pathogens of*
804 *Atlantic salmon: Lessons from *Gyrodactylus salaris**. *In Atlantic Salmon*
805 *Ecology*, pp. 221–252. Ed. by Ø. Aas, S. Einum, A. Klemetsen, and J. Skurdal.
806 Wiley-Blackwell, Chichester (UK). 496 pp.

807 Hays, G. C., Ferreira, L. C., Sequeira, A. M. M., Meekan, M. G., Duarte, C. M.,
808 Bailey, H., Bailleul, F., *et al.* 2016. *Key questions in marine megafauna*
809 *movement ecology*. *Trends in Ecology and Evolution*, 31: 463-475.

810 Hedger, R.D., Rikardsen, A.H., and Thorstad E.B. In press. *Pop-up satellite archival*
811 *tag effects on the diving behaviour, growth and survival of adult Atlantic salmon*
812 *at sea*. *Journal of Fish Biology*.

813 Hill, R. D., and Braun, M. J. 2001. *Geolocation by light level—The next step:*
814 *Latitude*. *In Electronic Tagging and Tracking in Marine Fisheries*, pp. 315–330.

815 Ed. by J. R. Sibert and J. L. Nielsen. Springer, Netherlands. 468 pp.

816 Howey-Jordan, L. A., Brooks, E. J., Abercrombie, D. L., Jordan, L. K. B., Brooks, A.,
817 Williams, S., Gospodarczyk, E., *et al.* 2013. Complex movements, philopatry
818 and expanded depth range of a severely threatened pelagic shark, the Oceanic
819 whitetip (*Carcharhinus longimanus*) in the Western North Atlantic. PLoS ONE,
820 8: e56588

821 ICES. 2015. Report of the Working Group on North Atlantic Salmon (WGNAS).
822 ICES Document CM 2015/ACOM:09. 332 pp.

823 Jacobsen, J. A., Hansen, L. P., Bakkestuen, V., Halvorsen, R., Reddin, D. G., White,
824 J., O Maoileidigh, N., *et al.* 2012. Distribution by origin and sea age of Atlantic
825 salmon (*Salmo salar*) in the sea around the Faroe Islands based on analysis of
826 historical tag recoveries. ICES Journal of Marine Science, 69: 1598–1608.

827 Jensen, A. J., Karlsson, S., Fiske, P., Hansen, L. P., Østborg, G. M., and Hindar, K.
828 2014. Origin and life history of Atlantic salmon (*Salmo salar*) near their
829 northernmost oceanic limit. Canadian Journal of Fisheries and Aquatic Sciences,
830 71: 1740-1746

831 Krkosek, M., Revie, C. W., Gargan, P. G., Skilbrei, O. T., Finstad, B., and Todd, C.
832 D. 2013. Impact of parasites on salmon recruitment in the Northeast Atlantic
833 Ocean. Proceedings of the Royal Society: Biological Sciences, 280: 20122359.

834 Lacroix, G. L. 2013. Population-specific ranges of oceanic migration for adult
835 Atlantic salmon (*Salmo salar*) documented using pop-up satellite archival tags.
836 Canadian Journal of Fisheries and Aquatic Sciences, 70: 1011–1030.

837 Lea, J. S. E., Wetherbee, B. M., Queiroz, N., Burnie, N., Aming, C., Sousa, L. L.,
838 Mucientes, G. R., *et al.* 2015. Repeated, long-distance migrations by a
839 philopatric predator targeting highly contrasting ecosystems. Scientific Reports,

840 5: 11202.

841 McCarthy, J. L., Friedland, K. D., and Hansen, L. P. 2008. Monthly indices of the
842 post-smolt growth of Atlantic salmon from the Drammen River, Norway. *Journal*
843 *of Fish Biology*, 72: 1572–1588.

844 Miller, A. S., Sheehan, T. F., Renkawitz, M. D., Meister, A. L., and Miller, T. J. 2012.
845 Revisiting the marine migration of US Atlantic salmon using historical Carlin tag
846 data. *ICES Journal of Marine Science*, 69: 1609–1615.

847 Mills, K. E., Pershing, A. J., Sheehan, T. F., and Mountain, D. 2013. Climate and
848 ecosystem linkages explain widespread declines in North American Atlantic
849 salmon populations. *Global Change Biology*, 19: 3046–3061.

850 Musyl, M. K., Brill, R. W., Curran, D. S., Gunn, J. S., Hartog, J. R., Hill, R. D.,
851 Welch, D. W., *et al.* 2001. Ability of Archival Tags to Provide Estimates of
852 Geographical Position Based on Light Intensity. *In* *Electronic Tagging and*
853 *Tracking in Marine Fisheries*, pp. 343–367. Ed. by J.R. Sibert and J.L. Nielsen.
854 Springer, Netherlands. 468 pp.

855 Neilson, J. D., Loefer, J., Prince, E. D., Royer, F., Calmettes, B., Gaspar, P., Lopez,
856 R., *et al.* 2014. Seasonal distributions and migrations of Northwest Atlantic
857 swordfish: Inferences from integration of pop-up satellite archival tagging
858 Studies. *PLoS ONE*, 9: e112736.

859 Nielsen, A., Bigelow, K. A., Musyl, M. K., and Sibert, J. R. 2006. Improving light-
860 based geolocation by including sea surface temperature. *Fisheries*
861 *Oceanography*, 15: 314–325.

862 Otero, J., Jensen, A. J., L'Abée-Lund, J. H., Stenseth, N. C., Storvik, G. O., and
863 Vøllestad, L. A. 2011. Quantifying the ocean, freshwater and human effects on
864 year-to-year variability of one-sea-winter Atlantic salmon angled in multiple

865 Norwegian rivers. PLoS ONE, 6: e24005

866 Parrish, D. L., Behnke, R. J., Gephard, S. R., McCormick, S. D., and Reeves, G. H.
867 1998. Why aren't there more Atlantic salmon (*Salmo salar*)? Canadian Journal
868 of Fisheries and Aquatic Sciences, 55: 281–287.

869 Pedersen, M. W. 2010. Hidden Markov modelling of movement data from fish. Ph.D.
870 thesis, Technical University of Denmark, Kongens Lyngby, Denmark. 188 pp.

871 Pedersen, M. W., Patterson, T. A., Thygesen, U. H., and Madsen, H. 2011. Estimating
872 animal behavior and residency from movement data. Oikos, 120: 1281–1290.

873 Pedersen, M. W., Righton, D., Thygesen, U. H., Andersen, K. H., and Madsen, H.
874 2008. Geolocation of North Sea cod (*Gadus morhua*) using hidden Markov
875 models and behavioural switching. Canadian Journal of Fisheries and Aquatic
876 Sciences, 65: 2367–2377.

877 R Core Team. 2015. R: A language and environment for statistical computing. R
878 Foundation for Statistical Computing; Vienna; Austria. [https://www.r-](https://www.r-project.org/)
879 [project.org/](https://www.r-project.org/).

880 Reddin, D. G., Downton, P., Fleming, I. A., Hansen, L. P., and Mahon, A. 2011.
881 Behavioural ecology at sea of Atlantic salmon (*Salmo salar* L.) kelts from a
882 Newfoundland (Canada) river. Fisheries Oceanography, 20: 174–191.

883 Reddin, D. G., Friedland, K. D., Downton, P., Dempson, J. B., and Mullins, C. C.
884 2004. Thermal habitat experienced by Atlantic salmon (*Salmo salar* L.) kelts in
885 coastal Newfoundland waters. Fisheries Oceanography, 13: 24–35.

886 Reddin, D. G., Hansen, L. P., Bakkestuen, V., Russel, I., White, J., Potter, E. C. E.
887 (Ted), Dempson, J. B., *et al.* 2012. Distribution and biological characteristics of
888 Atlantic salmon (*Salmo salar*) at Greenland based on the analysis of historical
889 tag recoveries. ICES Journal of Marine Science, 69: 1589–1597.

890 Reddin, D. G., and Short, P. B. 1991. Postsmolt Atlantic salmon (*Salmo salar*) in the
891 Labrador Sea. *Canadian Journal of Fisheries and Aquatic Sciences*, 48: 2–6.

892 Renkawitz, M. D., Sheehan, T. F., Dixon, H. J., and Nygaard, R. 2015. Changing
893 trophic structure and energy dynamics in the Northwest Atlantic: Implications
894 for Atlantic salmon feeding at West Greenland. *Marine Ecology Progress Series*,
895 538: 197–211.

896 Ritter, J. A. 1989. Marine migration and natural mortality of North American Atlantic
897 salmon (*Salmo salar* L.). *Canadian Manuscript Report of Fisheries and Aquatic*
898 *Sciences* No. 2041. 136 pp.

899 Sheehan, T. F., Reddin, D. G., Chaput, G., and Renkawitz, M. D. 2012. SALSEA
900 North America: a pelagic ecosystem survey targeting Atlantic salmon in the
901 Northwest Atlantic. *ICES Journal of Marine Science*, 69: 1580–1588.

902 Sibert, J. R., Musyl, M. K., and Brill, R. W. 2003. Horizontal movements of bigeye
903 tuna (*Thunnus obesus*) near Hawaii determined by Kalman filter analysis of
904 archival tagging data. *Fisheries Oceanography*, 12: 141–151.

905 Teo, S. L. H., Sandstrom, P. H., Chapman, E. D., Null, R. E., Brown, K., Klimley, A.
906 P., and Block, B. A. 2013. Archival and acoustic tags reveal the post-spawning
907 migrations, diving behaviour, and thermal habitat of hatchery-origin Sacramento
908 River steelhead kelts (*Oncorhynchus mykiss*). *Environmental Biology of Fishes*,
909 96: 175-187.

910 Thygesen, U. H., Pedersen, M. W., and Madsen, H. 2009. Geolocating fish using
911 Hidden Markov models and data storage tags. *In* *Tagging and Tracking of*
912 *Marine Animals with Electronic Devices*, pp. 277–293. Ed. by J. L. Nielsen, H.
913 Arrizabalaga, N. Fragoso, A. Hobday, M. Lutcavage, and J. Sibert. Springer,
914 Netherlands. 400 pp.

915 Viterbi, A. J. 2006. A personal history of the Viterbi algorithm. Signal Processing
916 Magazine, IEEE, 23: 120–142.
917
918
919